Type 2 Ryanodine Receptor Domain A Contains a Unique and Dynamic α-Helix That Transitions to a β-Strand in a Mutant Linked with a Heritable Cardiomyopathy

Fernando J. Amador[1], Lynn Kimlicka[2], Peter B. Stathopulos[1], Geneviève M.C. Gasmi-Seabrook[1], David H. MacLennan[3], Filip Van Petegem[2] and Mitsuhiko Ikura[1]

*1 - **Campbell Family Institute for Cancer Research,** Ontario Cancer Institute and Department of Medical Biophysics, University of Toronto, Toronto, Ontario, Canada M5G 1L7*
*2 - **Department of Biochemistry and Molecular Biology,** University of British Columbia, Vancouver, British Columbia, Canada V6T 1Z3*
*3 - **Banting and Best Department of Medical Research,** University of Toronto, Charles H. Best Institute, 112 College Street, Toronto, Ontario, Canada MSG 116*

***Correspondence to Filip Van Petegem and Mitsuhiko Ikura:** filip.vanpetegem@gmail.com; mikura@uhnres.utoronto.ca*
http://dx.doi.org/10.1016/j.jmb.2013.08.015
Edited by A. G. Palmer III

Abstract

Ryanodine receptors (RyRs) are large tetrameric calcium (Ca^{2+}) release channels found on the sarcoplasmic reticulum that respond to dihydropyridine receptor activity through a direct conformational interaction and/or indirect Ca^{2+} sensitivity, propagating sarcoplasmic reticulum luminal Ca^{2+} release in the process of excitation–contraction coupling. There are three human RyR subtypes, and several debilitating diseases are linked to heritable mutations in RyR1 and RyR2 including malignant hypothermia, central core disease, catecholaminergic polymorphic ventricular tachycardia (CPVT) and arrhythmogenic right ventricular dysplasia type 2 (ARVD2). Despite the recent appreciation that many disease-associated mutations within the N-terminal RyRABC domains (i.e., residues 1–559) are located in the putative interfaces mediating tetrameric channel assembly, the precise structural and dynamical consequences of the mutations are not well understood. We used solution nuclear magnetic resonance (NMR) spectroscopy and X-ray crystallography to examine the effect of ARVD2-associated (i.e., R176Q) and CPVT-associated [i.e., P164S, R169Q and delta exon 3 (Δ3)] mutations on the structure and dynamics of RyR2A. Our solution NMR data exposed a mobile α-helix, unique to type 2; further, this α2 helix rescues the β-strand lost in RyR2A Δ3 but remains dynamic in the hot-spot loop (HS-loop) P164S, R169Q and R176Q mutant proteins. Docking of our X-ray crystal/NMR hybrid structure into the RyR1 cryo-electron microscopy map revealed that this RyR2A α2 helix is in close proximity to dense "columns" projecting toward the channel pore. This is in contrast to the HS-loop mutations that cause structural changes largely localized to the intersubunit interface between adjacent ABC domains. Taken together, our data suggest that ARVD2 and CPVT mutations have at least two distinct structural consequences linked to channel dysfunction: perturbation of the HS-loop (i.e., domain A):domain B intersubunit interface and disruption of the communication between the N-terminal region and the channel domain.

Introduction

Calcium (Ca^{2+}) is a universal signaling messenger, controlling myriad cellular activities in all mammalian cells. Cells compartmentalize most intracellular Ca^{2+} in the sarcoplasmic/endoplasmic reticulum, where it is spatiotemporally released into the cytosol during signaling cascades. Sarcoplasmic/endoplasmic reticulum receptor operated channels responsible for moving Ca^{2+} from the lumen to the cytosol include the inositol 1,4,5 trisphosphate receptors (IP_3Rs), which are abundant in non-excitable cells, and the ryanodine receptors (RyRs), which are found more exclusively in electrically excitable cells. Dysfunction of Ca^{2+} release through these receptor operated channels can have devastating

Please cite this article as: Amador Fernando J., et al, Type 2 Ryanodine Receptor Domain A Contains a Unique and Dynamic α-Helix That Transitions to a β-Strand in a Mutant Linked with a ..., J Mol Biol (2013), http://dx.doi.org/10.1016/j.jmb.2013.08.015

physiological consequences as several heritable human diseases are associated with mutations of the three *RyR* genes. These include malignant hyperthermia [1,2] and central core disease [3,4] that are associated with *RyR1* mutations or catecholaminergic polymorphic ventricular tachycardia (CPVT) [5,6] and arrhythmogenic right ventricular dysplasia type 2 (ARVD2) [7], which are associated with *RyR2* mutations. Furthermore, recent studies have shown that overexpression of *RyR3* and alternative splicing of *RyR2* and *RyR3* may play a role in Alzheimer's disease [8,9].

RyRs form tetrameric complexes that are the largest known ion channels at ~2.2 MDa. They reside on the sarcoplasmic reticulum in close apposition to plasma membrane voltage-gated dihydropyridine receptor (DHPRs). RyRs play an integral role in excitation–contraction coupling in skeletal muscle cells and cardiomyocytes [10,11], as they propagate Ca^{2+} release from the sarcoplasmic reticulum in response to increased cytosolic Ca^{2+} levels caused by DHPR activity or through direct sensing of a voltage-dependent conformational change in DHPR. RyR1 is found primarily in skeletal muscle [12], RyR2 is found primarily in cardiac muscle [13] and RyR3 is found in several cell types but was originally discovered in brain cells [14]. Most disease-associated mutations render the channel hypersensitive to activating stimuli such as Ca^{2+} on either the luminal or the cytosolic side of the receptor.

Structural investigations of the tetrameric channel by cryo-electron microscopy (cryo-EM) [15–20] and folded domains by X-ray crystallography [21–27] have provided insight into how RyRs function and how disease-associated mutations might affect this function. A study by Tung *et al.* showed that the majority of mutations found within the first 559 residues of RyR1 (RyR1-ABC) are clustered at intersubunit and intrasubunit interfaces rather than being buried within the folded domain cores [25]. The "hot-spot" loop (HS-loop) is the location of over half the mutations found within the A domain of the RyR1 and forms an interface with domain B from an adjacent subunit. An investigation of the position of the RyR1-ABC region in open and closed cryo-EM maps suggests that this interface is severely altered during channel opening and acts as a brake on channel opening [28]. Another study investigated a mutation involving elements within the A domain that are deleted in a severe form of CPVT [23]. The removal of exon 3 in *RyR2* (RyR2A Δ3) results in a 35-residue deletion (N57-G91) that does not destabilize the protein or cause misfolding. Surprisingly, the β-trefoil fold of this domain is rescued by the transformation of the preceding region of unknown structure into the missing β-strand; moreover, this insertion increases the thermal stability [22,23]. Docking studies reveal that the deleted portion of RyR2 is at an interface with an electron dense region that connects to the transmembrane region of the receptor [23].

Despite progress in locating disease-associated mutations within the structurally resolved N-terminal RyR domains and relative to the tetrameric assembly of the channel, the structural and dynamical consequences of the mutations are not well understood. Here, we use solution nuclear magnetic resonance (NMR) spectroscopy and X-ray crystallography to examine the effect of ARVD2-associated (i.e., R176Q) and CPVT-associated (i.e., P164S, R169Q and delta exon 3) mutations on the structure and dynamics of RyR2A. Remarkably, our solution NMR data elucidated the presence of a previously unresolved α-helix in wild-type RyR2A; further, docking of our X-ray crystal/NMR hybrid structure into the cryo-EM map of RyR1 revealed that this helix resides in close proximity to electron dense "columns" projecting toward the channel pore. In solution, this α-helix rescues the β-strand deleted in RyR2A Δ3 but remains dynamic in HS-loop mutant proteins (i.e., P164S, R169Q and R176Q). Mutations in the HS-loop cause structural changes within the A domain largely localized to the loop itself, which presumably cause dysfunction *via* perturbation of intersubunit HS-loop:domain B interfaces. Our studies show that ARVD2 and CPVT mutations found in the A domain result in at least two different structural consequences that are presumably linked to the functional defects found in the mutated channels [29,30].

Results

RyR2A forms a dynamic α2 helix in solution

A construct encompassing residues 10–224 in mouse RyR2 was used in solution NMR experiments to assign the protein backbone atoms of RyR2A. Deuteration and transverse relaxation optimized spectroscopy (TROSY)-based experiments were implemented to ameliorate spectral crowding and broadened signals undergoing chemical exchange. Assignment of the $^{1}H–^{15}N$ TROSY–heteronuclear single quantum coherence (HSQC) spectrum was achieved for approximately 88% of observable cross-peaks (Fig. 1a).

A chemical shift index (CSI) plot derived from the present solution NMR C^{α} and C^{β} chemical shifts of RyR2A revealed a previously invisible α2 helix that is absent in the crystal structure of RyR2A (Fig. 1b). This supplementary helix spans a 10-residue stretch from V95 to T104 within a 12-residue insertion specific to the RyR2 sequence compared to RyR1 and RyR3 (Fig. 2a). All other secondary structural elements extracted from the CSI of RyR2A were in

Please cite this article as: Amador Fernando J., et al, Type 2 Ryanodine Receptor Domain A Contains a Unique and Dynamic α-Helix That Transitions to a β-Strand in a Mutant Linked with a ..., J Mol Biol (2013), http://dx.doi.org/10.1016/j.jmb.2013.08.015

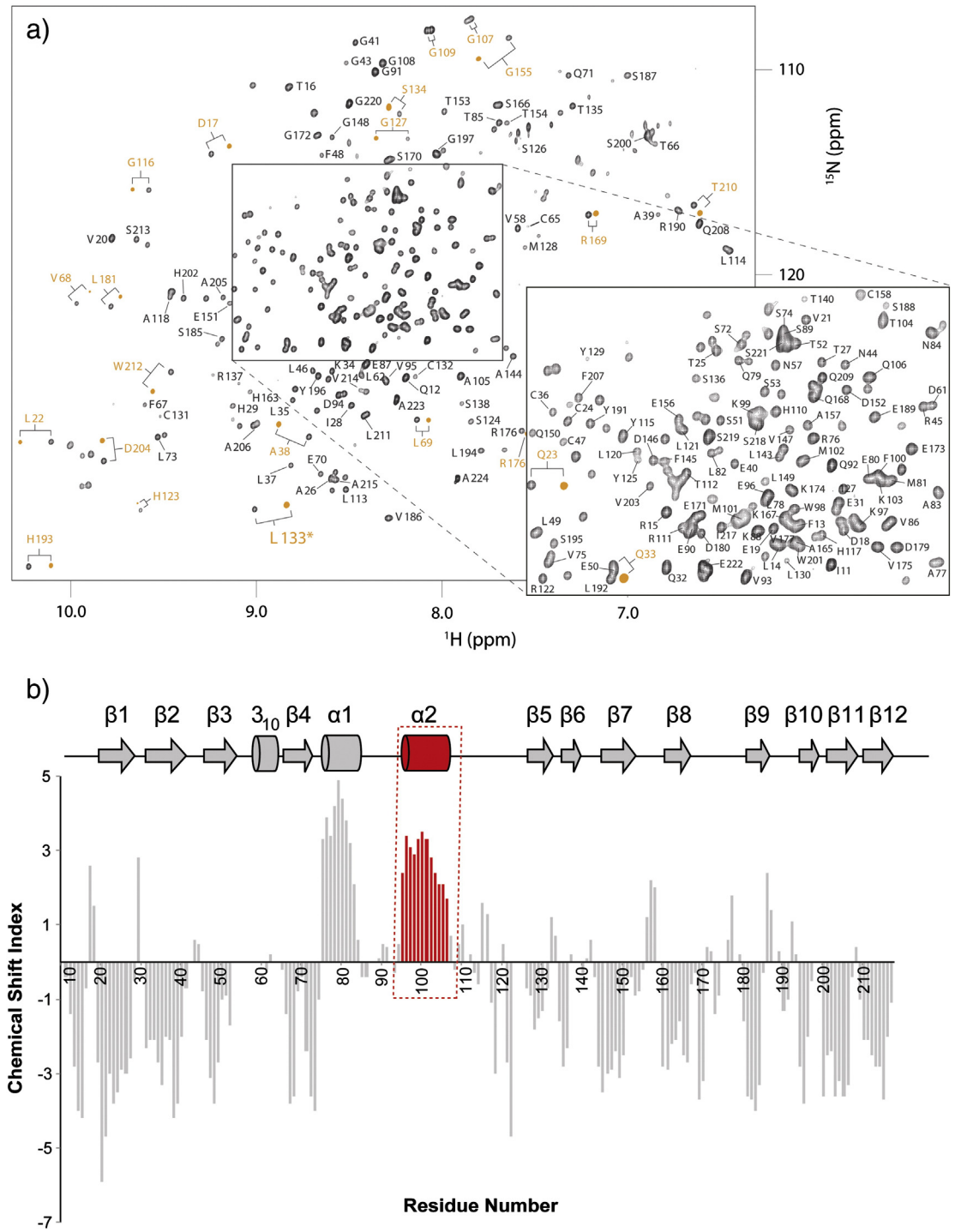

Fig. 1. Protein backbone assignment and CSI of RyR2A.(a) ^{1}H–^{15}N TROSY–HSQC spectrum of ^{15}N/^{13}C/^{2}H-labeled RyR2A 10–224. Assignment was achieved for 88% of the protein backbone. The inset shows a zoomed view of the crowded region of the HSQC. Cross-peaks connected by square brackets are derived from the same residue in two conformations (i.e., in chemical exchange) with orange peaks corresponding to the minor population. Peaks (L133, G155, H193 and W212) that were analyzed using zz-exchange spectroscopy experiments (Supplementary Fig. 1) are designated by an asterisk. (b) The CSI was generated using C^{α} and C^{β} chemical shifts of assigned residues. β-Strands, α-helices and random coils are indicated by large negative, large positive and small CSI values, respectively. Residues encompassing the newly discovered α2 helix are colored red. The secondary structure elements, which are derived only from the present solution NMR data (i.e., CSI), are shown above in cartoon format.

Please cite this article as: Amador Fernando J., et al, Type 2 Ryanodine Receptor Domain A Contains a Unique and Dynamic α-Helix That Transitions to a β-Strand in a Mutant Linked with a ..., J Mol Biol (2013), http://dx.doi.org/10.1016/j.jmb.2013.08.015

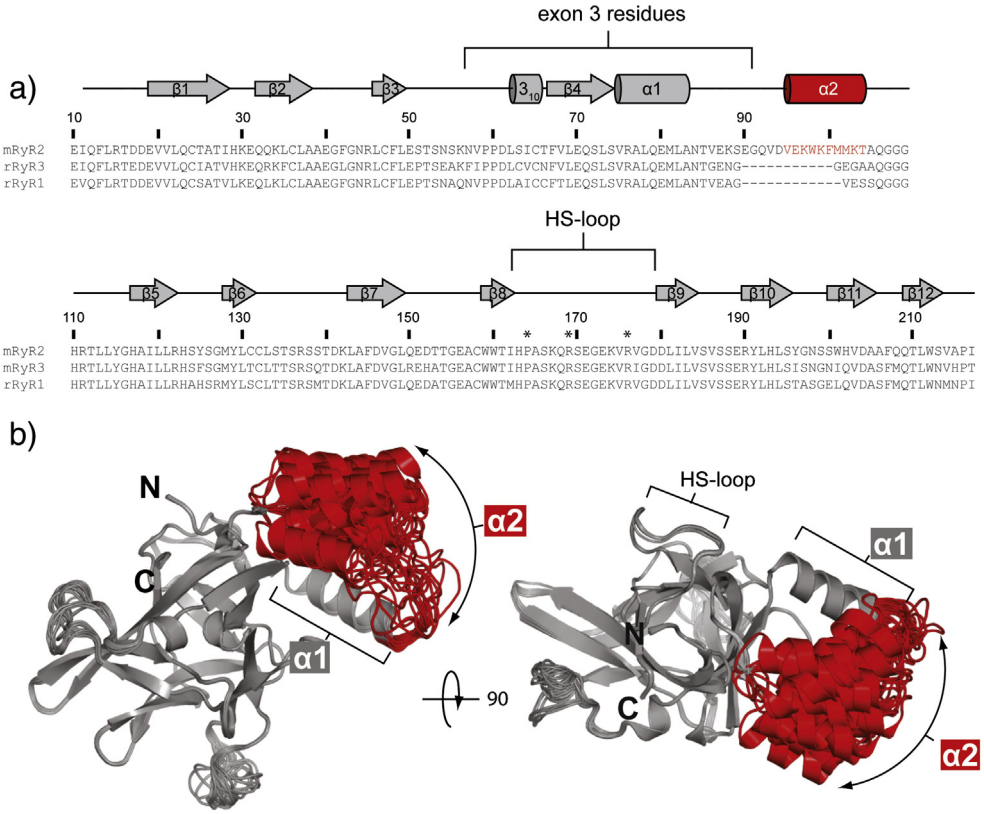

Fig. 2. X-ray crystallography/NMR hybrid model.(a) A sequence alignment for residues 10–217 demonstrates a high identity between RyR1A, RyR2A and RyR3A isoforms, with the exception of a 12-residue insertion, only present in RyR2. The location of exon 3 and HS-loop residues is shown. Asterisks denote the location of HS-loop mutations. Secondary structural elements derived from the X-ray crystallography/NMR hybrid structure are shown above the sequence. (b) The 20 lowest-energy backbone structures are shown for RyR2A. The newly identified α2 helix is colored red, and the HS-loop and α1 helix locations are indicated.

excellent agreement with the previously solved crystal structure [22].

The conservation of the number and location of secondary structural elements between RyR2A in solution and in the crystalline state allowed us to generate an X-ray crystallography/NMR hybrid model that includes the new α2 helix (Fig. 2b). The hybrid structure was calculated using hydrogen bond, torsion angle and distance restraints for the core RyR2A domain extracted from the crystal structure and combined with hydrogen bond and torsion angle restraints derived from the chemical shift data of RyR2A in solution. Alignment of the conserved secondary structure components of the 20 lowest-energy hybrid structures revealed that the location of the α2 helix exhibits a greater backbone RMSD compared to the remaining secondary structure elements (Fig. 2b). This increased variability is consistent with the assessment of dynamics for this region (see below).

In our previous study, we observed that a number of peaks in the RyR1 A domain (RyR1A) exhibited peak doubling in $^{1}H–^{15}N$ HSQC spectra [21]. In this study, we consistently observed peak doubling for a large number of cross-peaks in $^{1}H–^{15}N$ TROSY–HSQC spectra of wild-type and disease-related mutants, P164S, R169Q, R176Q and Δ3 (Fig. 1a and see below). To further test whether the peak doubling was due to chemical exchange caused by multiple protein conformations, we carried out a zz-exchange experiment on RyR2A that showed a build-up of exchange peak intensity and simultaneous decrease in auto peak intensity as a function of mixing time, thereby confirming the relatively slow chemical exchange phenomenon (Supplementary Fig. 1). We also observed a negligible change from low to moderately high temperatures on peak doubling (i.e., ~9–30 °C) (Supplementary Fig. 2a), suggesting that each conformation is moderately stable. Ultimately, we quantified the peak doubling by measuring the difference in the ^{1}H and ^{15}N chemical shifts between each doublet to obtain a delta omega (Δω) value (Supplementary Fig. 2b). Plotting a gradient of Δω values on our hybrid structure revealed that the highest values are concentrated

Please cite this article as: Amador Fernando J., et al, Type 2 Ryanodine Receptor Domain A Contains a Unique and Dynamic α-Helix That Transitions to a β-Strand in a Mutant Linked with a ..., J Mol Biol (2013), http://dx.doi.org/10.1016/j.jmb.2013.08.015

on the face of the structure where the newly identified α2 helix is located (Supplementary Fig. 2c). Since folding is a highly cooperative process for compact domains such as β-trefoils, the large Δω values concentrated on β-strands far from α2 (Supplementary Fig. 2c) could be caused by propagation from β4 to other regions of the trefoil core. Taken together, these data suggest that RyR2A slowly exchanges between two moderately stable conformations in solution and α2 undergoes the greatest change in chemical environment.

HS-loop mutations in RyR2A cause local perturbations in RyR2A structure

In order to investigate the structural impact of disease-associated mutations located within the HS-loop of RyR2, we solved the crystal structures of RyR2A mutants, P164S, R169Q and R176Q, to resolutions between ~2.15 and 2.55 Å (Supplementary Table 1). Because the conformation of the loop might be affected by crystal contacts and the wild-type RyR2A structure was solved in a different space group (*C*2), we compared these structures with the previously published A77V mutant [22], which crystallized in the same space group as the three hot-spot mutants. A77V is located far away from the HS-loop and is, therefore, not expected to impact the conformation of the loop.

Pro164 is located at the beginning of the HS-loop and presumably provides a degree of conformational rigidity to this loop. Mutating this residue to Ser likely results in partial flexibility, as a portion of the loop exhibits weak electron density (Supplementary Fig. 3a and b). The side chain of Arg169 also appears inherently flexible with poorly defined electron density and was not modeled in the A77V structure. In the R169Q mutant structure, several residues, including R169Q, were not visible in the electron density, consistent with the higher degree of flexibility (Supplementary Fig. 3c and d). The R176Q mutation facilitates the formation of a hydrogen bond between Gln176 and Arg169. This interaction also positions Arg169 for a salt bridge with Asp179; however, several neighboring residues still showed missing electron density (Supplementary Fig. 3e and f).

Although the HS-loops in the mutant proteins appear partially flexible, as indicated by poor electron density, crystal contacts may have affected the resolution of the loops. For example, in the wild-type RyR2A structure, which was crystallized in a different space group, the loop position is different from that of these mutant structures [22]. Although crystal contacts do not impart large structural changes, the conformations of loops that are inherently flexible can be particularly sensitive. Therefore, we performed more detailed solution NMR experiments to circumvent any effects by crystal contacts on the HS-loop properties.

The spectra of the P164S, R169Q and R176Q mutants were assigned by transference from wild-type RyR2A and using ^{15}N-resolved nuclear Overhauser enhancement (NOE) spectroscopy–TROSY data for peaks that did not coincide sufficiently between spectra. We examined the effect of the three HS-loop mutations on the structural fold of RyR2A, including the α2 helix by monitoring chemical shift perturbations (CSPs) (Supplementary Fig. 4a). Plotting the CSPs on the hybrid structure of RyR2A revealed distinct magnitudes of structural perturbations caused by each mutation (Fig. 3). The P164S mutation resulted in the largest CSPs for residues throughout HS-loop and for residues immediately adjacent to the HS-loop. The R169Q mutation had a moderate conformational effect on the HS-loop and the core structure, while the perturbation of R176Q was limited to the immediate vicinity of the substituted residue. It is noteworthy that no mutation-induced structural perturbations were observed in α2 despite the close proximity of the C-terminal region of α2 to the HS-loop (Fig. 2a and Supplementary Fig. 4b). Taken together, the data suggest that P164S, R169Q and R176Q cause local structural perturbations within or near the HS-loop, overall consistent with the crystal structure analyses.

Residues in the α2 region undergo fast internal motion

We acquired ^{15}N–{^{1}H} backbone relaxation data to probe the dynamics of RyR2A. Plots of the longitudinal (R1) and transverse relaxation (R2) rates and steady-state ^{15}N–{^{1}H} NOE reveal several areas of increased mobility. In particular, the N- and C-terminal regions and the loops flanking the α2 helix exhibit increased R1, decreased R2 and attenuated ^{15}N–{^{1}H} heteronuclear NOE ratios, indicative of increased mobility (Supplementary Fig. 5). The increased R1 and decreased ^{15}N–{^{1}H} NOEs suggest that these regions are undergoing fast dynamics on an approximate picosecond-to-nanosecond timescale (Supplementary Fig. 5). The P164S, R169Q and R176Q HS-loop mutants all exhibited very similar relaxation parameter profiles as the wild-type protein (data not shown).

We subjected the relaxation data for wild type and the P164S mutant that showed the greatest CSPs among the HS-loop mutants to a model-free analysis in order to obtain parameters describing the internal motion of the individual NH bond vectors (Fig. 4). The generalized order parameter, S^2, suggests that the majority of RyR2A is rigid with an average S^2 value of 0.86 ± 0.03; however, the two loops flanking α2 demonstrate high mobility on an approximate picosecond-to-nanosecond timescale as evidenced by their lower S^2 values (Fig. 4a). The internal correlation time (τ_e) extracted for residues 85–109

Please cite this article as: Amador Fernando J., et al, Type 2 Ryanodine Receptor Domain A Contains a Unique and Dynamic α-Helix That Transitions to a β-Strand in a Mutant Linked with a ..., J Mol Biol (2013), http://dx.doi.org/10.1016/j.jmb.2013.08.015

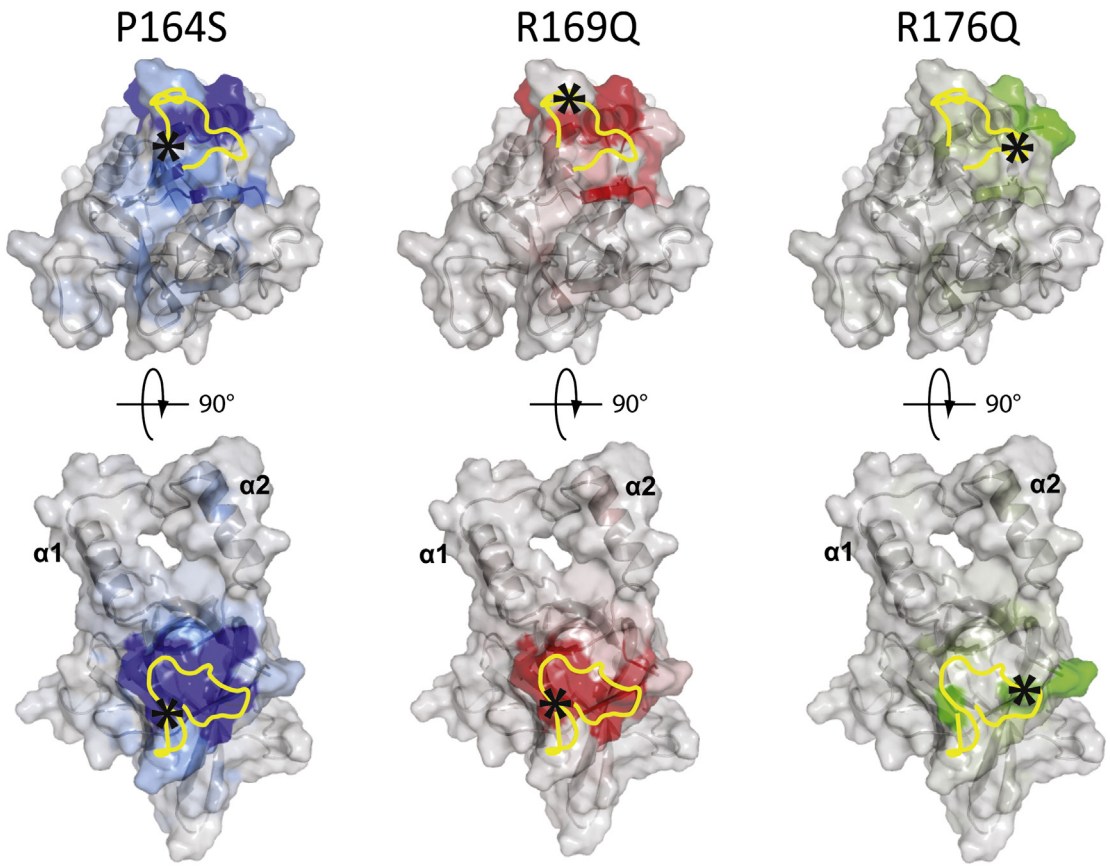

Fig. 3. CSPs on RyR2A caused by the disease-associated P164S, R169Q and R176Q mutations.CSPs generated by each HS-loop mutant are mapped onto the hybrid model of RyR2A. The P164S, R169Q and R176Q perturbations are shown in blue, red and green, respectively, and the HS-loop is outlined in yellow. An asterisk shows the site of each mutation.

(average of 15 ns), which correspond to α2 and the two loops flanking the helix, demonstrates that this entire region of RyR2A is undergoing fast internal motions on an approximate picosecond-to-nanosecond timescale compared to the overall rotational motion of the protein (Fig. 4b). The higher internal mobility of this region is consistent with the lack of electron density observed for α2 in any crystal structure of RyR2A and the variability observed in the position of α2 in our hybrid structure. The lack of systematically fitted and clustered R_{ex} values (Fig. 4c) suggests that the peak doubling (i.e., chemical exchange) phenomenon is on a slower timescale than the backbone relaxation experiments, corroborated by the zz-exchange experiments clearly demonstrating the exchange in a greater than millisecond timescale. Surprisingly, the P164S HS-loop mutation did not significantly alter the model-free parameters within the HS-loop or any other part of the structure compared to wild type (Fig. 4a and b). Overall, the NMR backbone relaxation data suggest that the globular domain of RyR2A is relatively rigid with the newly identified α2 helix and associated loop residues undergoing fast internal motion.

Exon 3 deletion induces an α2 helix-to-β4 transformation in RyR2A

In order to calculate the CSI of RyR2A Δ3, we required the relatively complete backbone assignment. The $^{1}H–^{15}N$ TROSY–HSQC for the RyR2A Δ3 protein was ~92% assigned using conventional three-dimensional backbone experiments, exhibiting a similar peak doubling/chemical exchange phenomenon as wild type (Supplementary Fig. 6). The CSI-derived secondary structure components were in excellent agreement with the previously solved crystal structure [23]. Comparison of the wild-type RyR2A with the RyR2A Δ3 CSI data provides evidence in solution for the rescue of the β-trefoil fold of RyR2A *via* the remarkable α-helix-to-β-strand switch (Fig. 5). We calculated the CSPs of RyR2A Δ3 relative to the wild-type spectrum and mapped them as a gradient on the wild-type structure, demonstrating that the conformational changes are localized

Please cite this article as: Amador Fernando J., et al, Type 2 Ryanodine Receptor Domain A Contains a Unique and Dynamic α-Helix That Transitions to a β-Strand in a Mutant Linked with a ..., J Mol Biol (2013), http://dx.doi.org/10.1016/j.jmb.2013.08.015

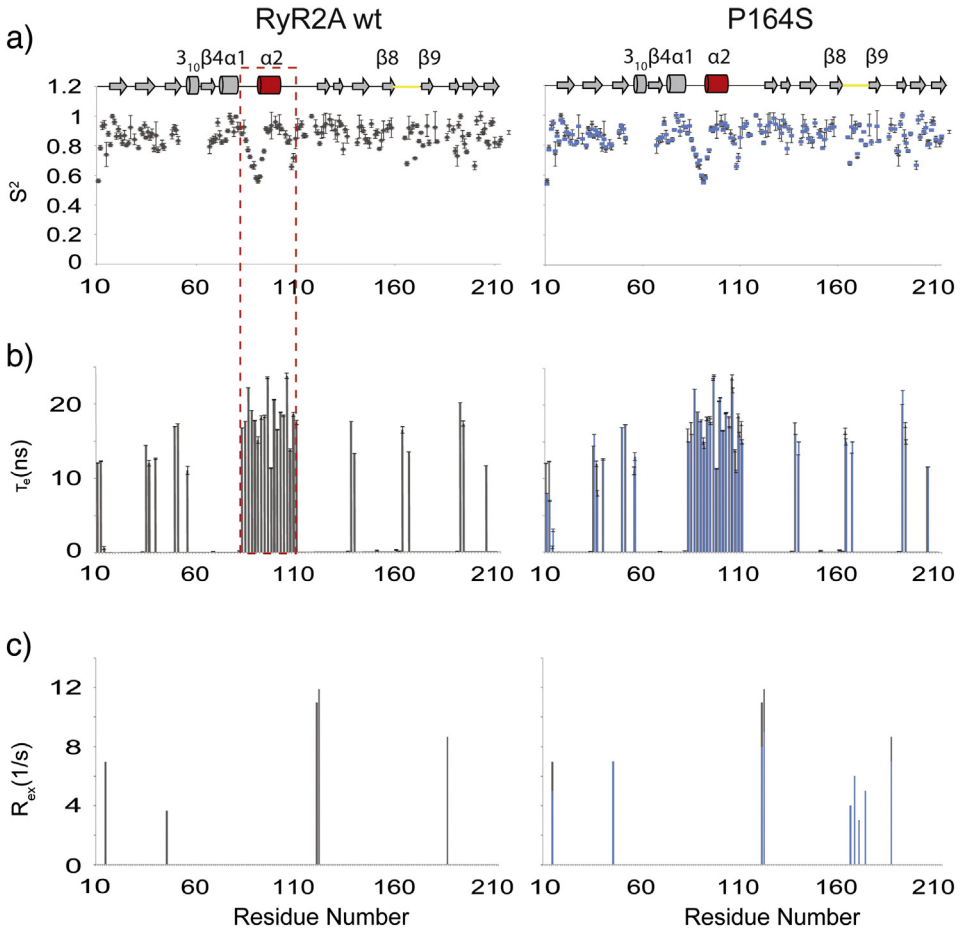

Fig. 4. Backbone dynamics of wild-type and P164S RyR2A.(a) Plot of generalized order parameter, S^2, derived from model-free analysis. Lower values indicate dynamic regions of the protein on a fast timescale (picosecond to nanosecond). (b) A plot of the internal correlation time, τ_e, outlines regions undergoing faster than average internal motions on an approximate picosecond-to-nanosecond timescale. (c) R_{ex} contributions are shown for residues undergoing slower internal motions (approximately microsecond to millisecond). Secondary structure elements for RyR2A are shown above. The mobile α2 region is outlined by a broken box.

to the region involved in the switch mechanism (Supplementary Fig. 7). Taken together, the RyR2A Δ3 solution NMR data suggest that the core β-trefoil fold remains largely unaltered despite the drastic change in primary structure.

Backbone dynamics parameters were also obtained for RyR2A Δ3 (Supplementary Fig. 8). RyR2A Δ3 remains a relatively rigid protein with an average S^2 of 0.87 ± 0.2. However, in the case of this deletion mutant, the loops flanking the rescued β4 strand exhibited increased dynamics on fast timescales (i.e., elevated R1 and decreased ^{15}N–{^{1}H} NOEs). Increased mobility of residues in the loop immediately after β4 (i.e., residues 104–109) as indicated by systematically lower S^2 values compared to RyR2A was observed. The consistently fitted τ_e values for residues 104–109 suggests that this loop also undergoes fast internal motions relative to the global tumbling; further, the lack of fast internal mobility for the rescued β4 is consistent with this strand robustly stabilizing the trefoil structure as a result of the exon 3 deletion.

Discussion

Mutation-driven structural alterations in the N-terminal region of RyR1 have been implicated in malignant hypothermia and central core disease pathophysiologies [25], in which the Ca^{2+} gating function of RyR1 is compromised. We previously suggested that the three key domains of the N-terminal region are dynamically intermolecularly and intramolecularly interacting with each other and that the mutations may affect this interplay required for the gating function of RyR1 [25,28]. In the present study, we employed NMR and X-ray approaches to investigate RyR2A, a cardiac isoform of the RyR proteins, which

Please cite this article as: Amador Fernando J., et al, Type 2 Ryanodine Receptor Domain A Contains a Unique and Dynamic α-Helix That Transitions to a β-Strand in a Mutant Linked with a ..., J Mol Biol (2013), http://dx.doi.org/10.1016/j.jmb.2013.08.015

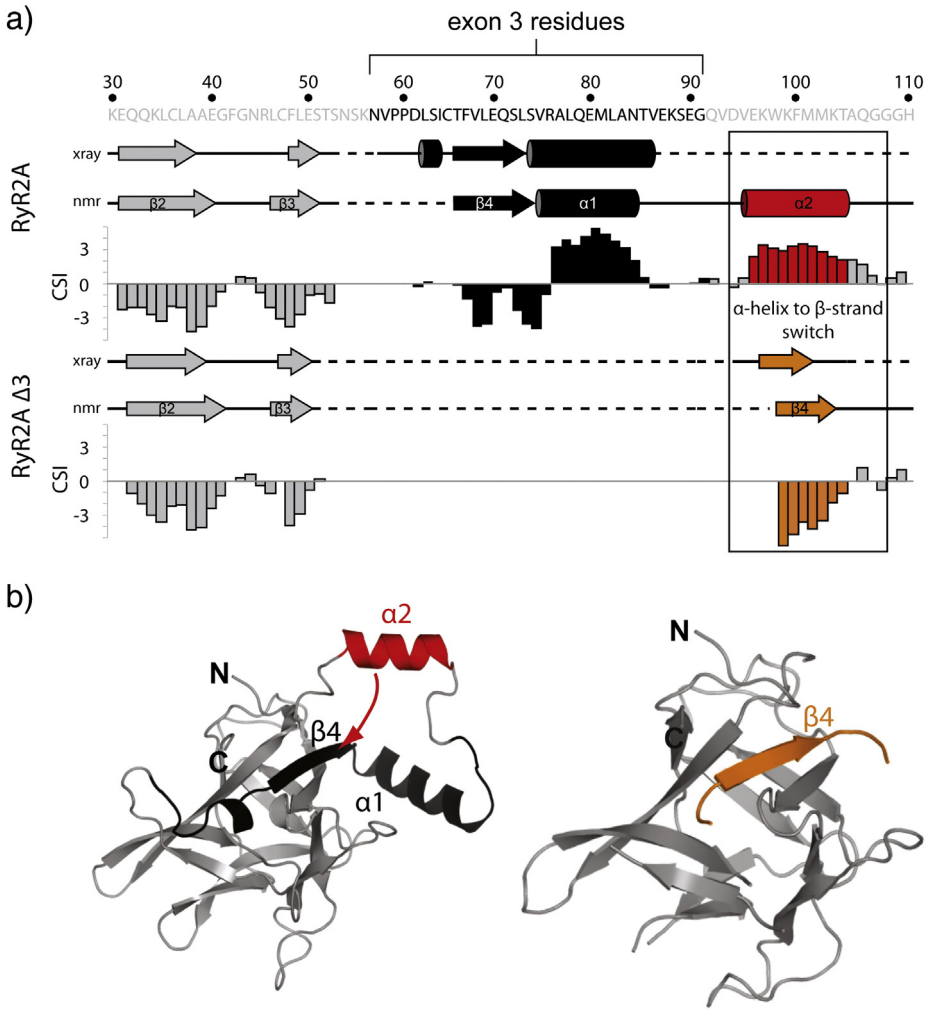

Fig. 5. Rescue of β-trefoil fold in solution by the α2-to-β4 switch in RyR2A Δ3.Solution NMR evidence of an α2 helix-to-β-strand switch as a consequence of exon 3 deletion. Residues in exon 3 are colored black in the sequence. Cartoon representation of the secondary structural elements is derived from X-ray crystallography structures and solution-based NMR methods. CSI values are plotted for both wild-type RyR2A and RyR2A Δ3. (b) Important structural elements involved in the α2 helix-to-β-strand switch are highlighted in the hybrid model of RyR2A (right panel). The rescued β4 strand is shown in the crystal structure of RyR2A Δ3 (right panel) (PDB ID: 3QR5).

possesses a unique insertion in the A domain (Fig. 2a). We show that the 12-residue insertion in RyR2A forms a mobile α2 helix, not detected in the X-ray structure of RyR2A due to its mobility [22]. Our previous NMR study on RyR1A established that a similar α2 helix does not form in the type 1 homologue [21]; moreover, the absence of the α2 helix in RyR1A and in RyR3A is consistent with deletion of the α2 forming residues in the RyR1A and RyR3A primary sequences (Fig. 2a). Interestingly, a structurally analogous helix within a similar helix–turn–helix motif is found in the suppressor domain of IP_3R1 despite a low sequence identity with RyR2A [31]. Structural alignment of our hybrid RyR2A structure with the IP_3R1 suppressor domain demonstrates that the longer helix in IP_3R pivots closer to the α1 helix than the range of orientations determined for the present RyR2A hybrid structure (Supplementary Fig. 9).

Previous docking studies highlighted two intermolecular interfaces involving domain A [23,25]. In the first interface, the HS-loop of domain A is modeled in close apposition to domain B of an adjacent subunit (Fig. 6) [23]. The exact position of the domains across this intersubunit interface differs between open and closed RyRs, and it is likely that the interactions are significantly altered during channel opening [25,28]. The precise conformation of the HS-loop would, therefore, play a critical role in defining this interface. Crystallographic, cryo-EM and NMR data of the HS-loop suggest that it is relatively rigid. Specifically, it is visible in the isolated

Please cite this article as: Amador Fernando J., et al, Type 2 Ryanodine Receptor Domain A Contains a Unique and Dynamic α-Helix That Transitions to a β-Strand in a Mutant Linked with a ..., J Mol Biol (2013), http://dx.doi.org/10.1016/j.jmb.2013.08.015

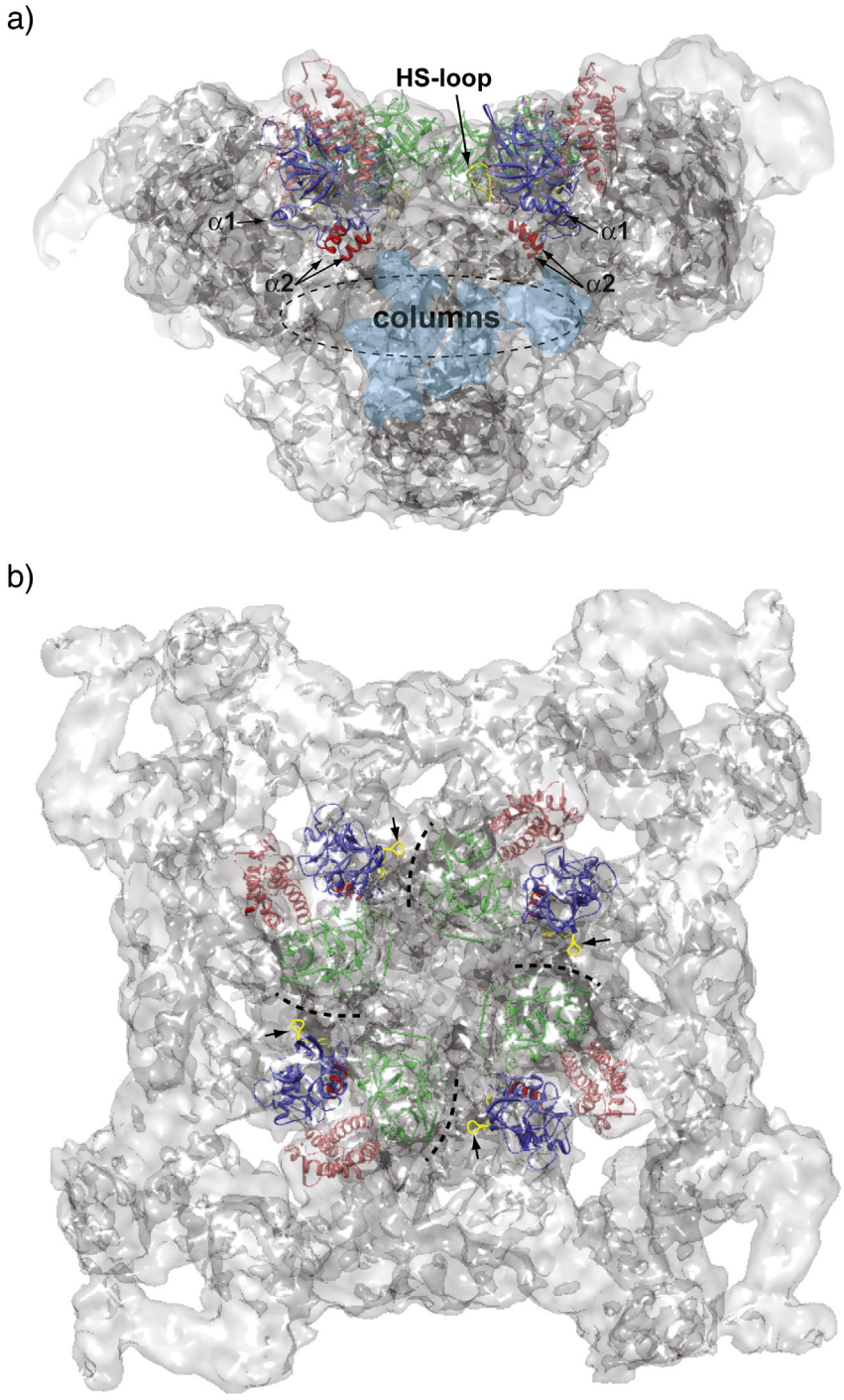

Fig. 6. Location of the RyR2A hybrid structure in the tetrameric cryo-EM map of full-length RyR1.(a) Side view of the RyR2A hybrid model (blue) superimposed with the RyR1-ABC structure (PDB ID: 2XOA) docked on the 9.6-Å cryo-EM map of "closed" RyR1 (EMDB code 1275). The B (green) and C (pink) domains from the N-terminal of RyR1-ABC are also shown. Black arrows indicate the location of the α1 helix and α2 helix, which is colored red for clarity. The electron dense columns are shaded cyan and outlined by a broken oval. (b) Top view of the docked RyR2A hybrid model. Small black arrows indicate the location of the HS-loop region that is shown in yellow. The interface between A and B is indicated by a broken line.

A domain of wild-type RyR1 [21] and RyR2 [22] and in RyR1-ABC [25] crystal structures, exhibiting low backbone RMSD among structures; further, backbone dynamic parameters of RyR2A are consistent with this rigidity (Fig. 4). Additionally, the docking of RyR1-ABC into the tetrameric full-length receptor

Please cite this article as: Amador Fernando J., et al, Type 2 Ryanodine Receptor Domain A Contains a Unique and Dynamic α-Helix That Transitions to a β-Strand in a Mutant Linked with a ..., J Mol Biol (2013), http://dx.doi.org/10.1016/j.jmb.2013.08.015

implies restricted mobility due to steric limitations (i.e., from the close apposition to domain B). The CSPs observed for the HS-loop mutants are primarily localized near the site of the mutation, and only marginal global structure, stability and backbone dynamics changes are observed for these mutant proteins, suggesting that local mutation-induced alterations to the HS-loop may perturb this important interface in disease-associated dysfunction.

The second interface is modeled between the α1 helix region of domain A and other RyR domains not yet structurally elucidated at high resolution [23]. In order to find the location of the RyR2A α2 helix in the tetrameric RyR structure, we first docked the RyR1-ABC structure onto the map of tetrameric RyR1 using the same unbiased protocol applied by Yuchi *et al.* [26]. Subsequently, we superimposed our hybrid structure onto the A domain of the docked RyR1-ABC structure (Fig. 6a). In this orientation, the α2 helix projects away from the cytosol and is in close apposition to the electron dense region, previously designated a "column" that extends toward the transmembrane region [17,20]. The α2 helix, which is adjacent to α1, is the closest structural element to the electron dense column connected to the pore (Fig. 6a). Interestingly, the α2 helix of the IP_3R1 suppressor domain also projects toward the transmembrane region in cryo-EM docking studies [32,33]. Thus, it is tempting to speculate that α2 interacts with a downstream RyR2 segment in the electron dense region in one of several interactions, including those mediated by α1, that connect the pore to the N-terminal domain. While this interaction may render the α2 helix less dynamic compared to the isolated RyR2A domain, the mobile nature of α2 suggests an intrinsic ability to move, and this movement may have important regulatory consequences for the channel. The α2 helix interaction may be specific for RyR2, conferring a distinct mode of channel regulation compared to RyR1 or RyR3. The peak doubling indicates chemical exchange on a slow timescale, suggesting that the isolated RyR2A domain accesses at least two conformations of similar stability; further, the ability to access two similarly stable conformations may be related to an ancillary mode of regulating the channel specific to RyR2 since peak doubling is not observed for RyR1A.

In the RyR2A Δ3 mutant protein, the α2 helix is transformed into a β-strand and sequestered in the β-trefoil fold. This structural conversion preserves wild-type-like rigidity in the β-trefoil core, consistent with an energetically favorable α2-to-β4 transition [23]. When the RyR2A Δ3 is studied in isolation, structural perturbations associated with this deletion mutation are limited to the regions involved in the motif conversion. However, our cryo-EM docking revealed that the location of the α2, which is omitted in the exon 3 deletion mutant, coincides with the interface between the mutation-rich N-terminal region and the "column" density immediately above the transmembrane channel region (Fig. 6a). These observations strongly argue that the exon 3 deletion may affect the communication between the N-terminal region and the channel domain *via* the "column" density identified in the cryo-EM structure. Consistent with this notion, a recent study revealed the functional consequences of removing the 35 residues in exon 3 on Ca^{2+} release termination [30], which is a critical step in excitation–contraction coupling and controlling cytosolic Ca^{2+} transients. Tang *et al.* demonstrated that RyR2 with the exon 3 deletion has a reduced luminal Ca^{2+} threshold for Ca^{2+} release termination and increased fractional Ca^{2+} release [30]. Considering the aforementioned structural analyses, we suggest that these functional observations are due to the uncoupling of a conformational linkage between the luminal Ca^{2+} sensing [34,35] function and the cytoplasmic regulatory function, part of which is played by the N-terminal region where numerous mutations including the exon 3 deletion have been identified.

Taken together, our data suggest that the HS-loop and the RyR2A Δ3 mutations are detrimental through a disturbance of the interfaces facilitated by the formation of the tetrameric receptor and/or regions involved in the allosteric regulation of the receptor, rather than a global conformational destabilization or structural change of domain A. Consistent with this notion, the mutant RyR2A proteins show a conservation in the backbone dynamics with wild type, and the structural perturbations are limited to the sites of mutation modeled in the interfaces through docking experiments. Further, high-resolution structural analyses are needed to elucidate the precise mechanisms of interface perturbation and the allosteric dysfunction they cause in disease states.

Materials and Methods

Protein expression and purification of NMR samples

Cloning, expression and purification of mouse RyR2A (10–224), HS-loop mutants (P164S, R169Q and R176Q) and RyR2A Δ3 (10–217) were carried out as in Amador *et al.* [21].

X-ray crystallography

Cloning, expression and purification of mouse RyR2A (residues 1–217) HS-loop mutants (P164S, R169Q and R176Q) for crystallography were performed as previously described [22]. All crystals were obtained by the hanging-drop vapor diffusion method using conditions described previously for RyR2A mutants [22]. Data collection statistics

Please cite this article as: Amador Fernando J., et al, Type 2 Ryanodine Receptor Domain A Contains a Unique and Dynamic α-Helix That Transitions to a β-Strand in a Mutant Linked with a ..., J Mol Biol (2013), http://dx.doi.org/10.1016/j.jmb.2013.08.015

are available in Supplementary Table 1. Molecular replacement was performed using Phaser [36] with a modified structure of RyR2A A77V (PDB ID: 3IM7) as a starting model, in which the HS-loop was deleted to remove bias. The models were completed by successive rounds of manual model building in Coot [37,38] and refinement with PHENIX [39]. The final refinement statistics can be found in Supplementary Table 1.

Backbone assignment of RyR2A and its disease-associated mutants

Protein samples for NMR backbone analyses contained 0.4 mM and 0.6 mM uniformly $^{15}N/^{13}C/^{2}H$-labeled wild-type and disease-associated mutant RyR2A, respectively. NMR buffers consisted of 20 mM sodium phosphate (pH 7.0), 300 mM NaCl, 5 mM DTT and 2 mM tris(2-carboxyethyl)phosphine for wild-type and HS-loop mutant RyR2A and of 20 mM sodium phosphate (pH 7.4), 300 mM NaCl, 5 mM DTT and 2 mM tris(2-carboxyethyl) phosphine for RyR2A Δ3. All samples contained 10% (v/v) D_2O. All experiments were carried out at 288 K on an 800-MHz Bruker spectrometer equipped with a cryogenically cooled triple resonance probe. Experimental setup, spectral processing and resonance assignment were carried out as previously described [21]. In addition, ^{15}N-edited three-dimensional NOE spectroscopy–TROSY [40] spectra were recorded for P164S and R169Q to aid with backbone assignment.

X-ray crystallography/NMR hybrid model

Restraints for backbone ϕ and ψ torsion angles and hydrogen bonds for the mobile α2 region (i.e., residues 85–109) were derived from the backbone chemical shifts using TALOS [41]. Coordinates from the RyR2A crystal structure (PDB ID: 3IM5) were used to generate restraints for the remaining residues of RyR2A. Both sets of restraints were combined and used to anneal an extended polypeptide chain in CNS [42] using the RECOORD scripts [43]. The 20 lowest-energy models out of 200 were chosen as a representative ensemble.

^{15}N Relaxation analysis

^{15}N Relaxation data were collected on all samples at 282 K, employing TROSY versions of the T1, T2 and ^{15}N–$\{^{1}H\}$ NOE pulse sequences [44]. Relaxation delays for RyR2A and the HS-loop mutants were as follows: T1: 10, 100, 400, 800 × 2, 1200 and 1600 ms; T2: 0, 15.84 × 2, 31.68, 47.52, 63.36, 79.2 and 95.04 ms. Delays used for RyR2A Δ3 were as follows: T1: 10, 100 × 2, 200, 500, 1000, 1200 and 1600 ms; T2: 0, 15.84 × 2, 31.68, 47.52, 63.36 and 79.2 ms. Duplicate spectra were used to estimate experimental error. Peak intensities were measured using SPARKY (University of California, San Francisco). ^{15}N–$\{^{1}H\}$ NOE experiments were carried out in the presence and absence of a 3-s proton saturation period before the ^{15}N excitation pulse. Peak intensity uncertainties were estimated from the noise level of the two spectra. Relaxation rates and heteronuclear NOE ratios were determined using the program Relax [45,46]. The relaxation data were analyzed according to the model-free approach of Lipari and Szabo [47,48] using TENSOR2 [49].

Cryo-EM docking

The RyR2A hybrid structure was superimposed onto the A domain of RyR1-ABC docked onto three different RyR1 cryo-EM maps (EMDB codes 1275, 1606 and 1607) as previously described [25].

Accession numbers

The coordinates and structure factors of the crystal structures have been deposited in the Research Collaboratory for Structural Bioinformatics database with PDB accession codes 4KEI for P164S, 4KEJ for R169Q and 4KEK for R176Q. The X-ray crystallography/NMR hybrid structural ensemble has been deposited in the Research Collaboratory for Structural Bioinformatics database with PDB accession code 2MC2, and the chemical shift assignments have been deposited in the Biological Magnetic Resonance Bank with accession codes 19424 and 19425.

Acknowledgements

This work was supported by Heart and Stroke Foundation of Canada, Canadian Institutes of Health Research and Natural Sciences and Engineering Research Council of Canada. The NMR facility at the University Health Network/Ontario Cancer Institute was funded by Campbell Family Institute. F.J.A. holds a Frederick Banting and Charles Best Graduate Scholarship Doctoral Award. M.I. holds the Canada Research Chair in Cancer Structural Biology. F.V.P. is a Michael Smith Foundation of Health Research Career Investigator.

Appendix A. Supplementary Data

Supplementary data to this article can be found online at http://dx.doi.org/10.1016/j.jmb.2013.08.015.

Received 24 April 2013;
Received in revised form 9 August 2013;
Accepted 19 August 2013
Available online xxxx

Keywords:
NMR;
crystallography;
calcium channel;
disease mutation;
protein dynamics

Abbreviations used:
CPVT, catecholaminergic polymorphic ventricular tachycardia; ARVD2, arrhythmogenic right ventricular dysplasia type 2; HS-loop, hot-spot loop; cryo-EM, cryo-electron microscopy; TROSY, transverse relaxation optimized spectroscopy; HSQC, heteronuclear single quantum coherence; CSI, chemical shift index; CSP, chemical shift perturbation; NOE, nuclear Overhauser enhancement.

References

[1] Jurkat-Rott K, McCarthy T, Lehmann-Horn F. Genetics and pathogenesis of malignant hyperthermia. Muscle Nerve 2000;23:4–17.

[2] MacLennan DH, Phillips MS. Malignant hyperthermia. Science 1992;256:789–94.

[3] Avila G, Dirksen RT. Functional effects of central core disease mutations in the cytoplasmic region of the skeletal muscle ryanodine receptor. J Gen Physiol 2001;118:277–90.

[4] Jungbluth H. Central core disease. Orphanet J Rare Dis 2007;2:25.

[5] Laitinen PJ, Brown KM, Piippo K, Swan H, Devaney JM, Brahmbhatt B, et al. Mutations of the cardiac ryanodine receptor (RyR2) gene in familial polymorphic ventricular tachycardia. Circulation 2001;103:485–90.

[6] Lehnart SE, Wehrens XH, Laitinen PJ, Reiken SR, Deng SX, Cheng Z, et al. Sudden death in familial polymorphic ventricular tachycardia associated with calcium release channel (ryanodine receptor) leak. Circulation 2004;109:3208–14.

[7] El Masry HZ, Yadav AV. Arrhythmogenic right ventricular dysplasia/cardiomyopathy. Expert Rev Cardiovasc Ther 2008;6:249–60.

[8] Bruno AM, Huang JY, Bennett DA, Marr RA, Hastings ML, Stutzmann GE. Altered ryanodine receptor expression in mild cognitive impairment and Alzheimer's disease. Neurobiol Aging 2012;33:e1–6.

[9] Berridge MJ. Calcium signalling and Alzheimer's disease. Neurochem Res 2011;36:1149–56.

[10] Dulhunty AF, Haarmann CS, Green D, Laver DR, Board PG, Casaratto MG. Interactions between dihydropyridine receptors and ryanodine receptors in striated muscle. Prog Biophys Mol Biol 2002;79:45–75.

[11] Rios E, Brum G. Involvement of dihydropyridine receptors in excitation-contraction coupling in skeletal muscle. Nature 1987;325:717–20.

[12] Zorzato F, Fujii J, Otsu K, Phillips M, Green NM, Lai FA, et al. Molecular cloning of cDNA encoding human and rabbit forms of the Ca^{2+} release channel (ryanodine receptor) of skeletal muscle sarcoplasmic reticulum. J Biol Chem 1990;265:2244–56.

[13] Nakai J, Imagawa T, Hakamat Y, Shigekawa M, Takeshima H, Numa S. Primary structure and functional expression from cDNA of the cardiac ryanodine receptor/calcium release channel. FEBS Lett 1990;271:169–77.

[14] Giannini G, Conti A, Mammarella S, Scrobogna M, Sorrentino V. The ryanodine receptor/calcium channel genes are widely and differentially expressed in murine brain and peripheral tissues. J Cell Biol 1995;128:893–904.

[15] Ludtke SJ, Serysheva II, Hamilton SL, Chiu W. The pore structure of the closed RyR1 channel. Structure 2005;13:1203–11.

[16] Radermacher M, Rao V, Grassucci R, Frank J, Timerman AP, Fleischer S, et al. Cryo-electron microscopy and three-dimensional reconstruction of the calcium release channel/ryanodine receptor from skeletal muscle. J Cell Biol 1994;127:411–23.

[17] Samso M, Feng W, Pessah IN, Allen PD. Coordinated movement of cytoplasmic and transmembrane domains of RyR1 upon gating. PLoS Biol 2009;7:e85.

[18] Samso M, Wagenknecht T, Allen PD. Internal structure and visualization of transmembrane domains of the RyR1 calcium release channel by cryo-EM. Nat Struct Mol Biol 2005;12:539–44.

[19] Serysheva II, Orlova EV, Chiu W, Sherman MB, Hamilton SL, van Heel M. Electron cryomicroscopy and angular reconstitution used to visualize the skeletal muscle calcium release channel. Nat Struct Biol 1995;2:18–24.

[20] Serysheva II, Ludtke SJ, Baker ML, Cong Y, Topf M, Eramian D, et al. Subnanometer-resolution electron cryomicroscopy-based domain models for the cytoplasmic region of skeletal muscle RyR channel. Proc Natl Acad Sci USA 2008;105:9610–5.

[21] Amador FJ, Liu S, Ishiyama N, Plevin MJ, Wilson A, MacLennan DH, et al. Crystal structure of type I ryanodine receptor amino-terminal β-trefoil domain reveals a disease-associated mutation "hot spot" loop. Proc Natl Acad Sci USA 2009;106:11040–4.

[22] Lobo PA, Van Petegem F. Crystal structures of the N-terminal domains of cardiac and skeletal muscle ryanodine receptors: insights into disease mutations. Structure 2009;17:1505–14.

[23] Lobo PA, Kimlicka L, Tung CC, Van Petegem F. The deletion of exon 3 in the cardiac ryanodine receptor is rescued by β strand switching. Structure 2011;19:790–8.

[24] Sharma P, Ishiyama N, Nair U, Li W, Dong A, Miyake T, et al. Structural determination of the phosphorylation domain of the ryanodine receptor. FEBS J 2012;279:3952–64.

[25] Tung CC, Lobo PA, Kimlicka L, Van Petegem F. The amino-terminal disease hotspot of ryanodine receptors forms a cytoplasmic vestibule. Nature 2010;468:585–8.

[26] Yuchi Z, Lau K, Van Petegem F. Disease mutations in the ryanodine receptor central region: crystal structures of a phosphorylation hot spot domain. Structure 2012;20:1201–11.

[27] Kimlicka L, Tung CC, Carlsson AC, Lobo PA, Yuchi Z, Van Petegem F. The cardiac ryanodine receptor N-terminal region contains an anion binding site that is targeted by disease mutations. Structure 2013;21:1440–9.

[28] Kimlicka L, Lau K, Tung CC, Van Petegem F. Disease mutations in the ryanodine receptor N-terminal region couple to a mobile intersubunit interface. Nat Commun 2013;4:1506.

[29] Kannankeril PJ, Mitchell BM, Goonasekera SA, Chelu MG, Zhang W, Sood S, et al. Mice with the R176Q cardiac ryanodine receptor mutation exhibit catecholamine-induced ventricular tachycardia and cardiomyopathy. Proc Natl Acad Sci USA 2006;103:12179–84.

[30] Tang Y, Tian X, Wang R, Fill M, Chen SR. Abnormal termination of Ca^{2+} release is a common defect of RyR2 mutations associated with cardiomyopathies. Circ Res 2012;110:968–77.

[31] Bosanac I, Yamazaki H, Matsu-Ura T, Michikawa T, Mikoshiba K, Ikura M. Crystal structure of the ligand binding suppressor domain of type 1 inositol 1,4,5-trisphosphate receptor. Mol Cell 2005;17:193–203.

Please cite this article as: Amador Fernando J., et al, Type 2 Ryanodine Receptor Domain A Contains a Unique and Dynamic α-Helix That Transitions to a β-Strand in a Mutant Linked with a ..., J Mol Biol (2013), http://dx.doi.org/10.1016/j.jmb.2013.08.015

[32] Seo MD, Velamakanni S, Ishiyama N, Stathopulos PB, Rossi AM, Khan SA, et al. Structural and functional conservation of key domains in InsP3 and ryanodine receptors. Nature 2012;483:108–12.
[33] Stathopulos PB, Seo MD, Enomoto M, Amador FJ, Ishiyama N, Ikura M. Themes and variations in ER/SR calcium release channels: structure and function. Physiology (Bethesda) 2012;27:331–42.
[34] Jiang D, Xiao B, Yang D, Wang R, Choi P, Zhang L, et al. RyR2 mutations linked to ventricular tachycardia and sudden death reduce the threshold for store-overload-induced Ca^{2+} release (SOICR). Proc Natl Acad Sci USA 2004;101: 13062–7.
[35] Laver DR. Ca^{2+} stores regulate ryanodine receptor Ca^{2+} release channels *via* luminal and cytosolic Ca^{2+} sites. Clin Exp Pharmacol Physiol 2007;34:889–96.
[36] McCoy AJ, Grosse-Kunstleve RW, Adams PD, Winn MD, Storoni LC, Read RJ. Phaser crystallographic software. J Appl Crystallogr 2007;40:658–74.
[37] Emsley P, Cowtan K. Coot: model-building tools for molecular graphics. Acta Crystallogr Sect D Biol Crystallogr 2004;60:2126–32.
[38] Emsley P, Lohkamp B, Scott WG, Cowtan K. Features and development of Coot. Acta Crystallogr Sect D Biol Crystallogr 2010;66:486–501.
[39] Adams PD, Afonine PV, Bunkoczi G, Chen VB, Davis IW, Echols N, et al. PHENIX: a comprehensive Python-based system for macromolecular structure solution. Acta Crystallogr Sect D Biol Crystallogr 2010;66:213–21.
[40] Zhu G, Kong XM, Sze KH. Gradient and sensitivity enhancement of 2D TROSY with water flip-back, 3D NOESY-TROSY and TOCSY-TROSY experiments. J Biomol NMR 1999;13:77–81.
[41] Shen Y, Delaglio F, Cornilescu G, Bax A. TALOS+: a hybrid method for predicting protein backbone torsion angles from NMR chemical shifts. J Biomol NMR 2009;44:213–23.
[42] Brunger AT, Adams PD, Clore GM, DeLano WL, Gros P, Grosse-Kunstleve RW, et al. Crystallography & NMR system: a new software suite for macromolecular structure determination. Acta Crystallogr Sect D Biol Crystallogr 1998;54:905–21.
[43] Nederveen AJ, Doreleijers JF, Vranken W, Miller Z, Spronk CA, Nabuurs SB, et al. RECOORD: a recalculated coordinate database of 500+ proteins from the PDB using restraints from the BioMagResBank. Proteins 2005;59:662–72.
[44] Zhu G, Xia Y, Nicholson LK, Sze KH. Protein dynamics measurements by TROSY-based NMR experiments. J Magn Reson 2000;143:423–6.
[45] d'Auvergne EJ, Gooley PR. Optimisation of NMR dynamic models II. A new methodology for the dual optimisation of the model-free parameters and the Brownian rotational diffusion tensor. J Biomol NMR 2008;40:121–33.
[46] d'Auvergne EJ, Gooley PR. Optimisation of NMR dynamic models. I. Minimisation algorithms and their performance within the model-free and Brownian rotational diffusion spaces. J Biomol NMR 2008;40:107–19.
[47] Lipari G, Szabo A. Model-free approach to the interpretation of nuclear magnetic resonance relaxation in macromolecules. 1. Theory and range of validity. J Am Chem Soc 1982;104: 4546–59.
[48] Lipari G, Szabo A. Model-free approach to the interpretation of nuclear magnetic resonance relaxation in macromolecules. 2. Analysis of experimental results. J Am Chem Soc 1982;104:4559–70.
[49] Dosset P, Hus JC, Blackledge M, Marion D. Efficient analysis of macromolecular rotational diffusion from heteronuclear relaxation data. J Biomol NMR 2000;16:23–8.

Please cite this article as: Amador Fernando J., et al, Type 2 Ryanodine Receptor Domain A Contains a Unique and Dynamic α-Helix That Transitions to a β-Strand in a Mutant Linked with a ..., J Mol Biol (2013), http://dx.doi.org/10.1016/j.jmb.2013.08.015